

A systems toxicology approach to identifying paracetamol overdose

Chantelle L. Mason^{*}, Joseph Leedale^{†,1}, Sotiris Tasoulis^{*}, Ian Jarman^{*}, Daniel J. Antoine^{‡,2},
Steven D. Webb^{*,2}

^{*}Department of Applied Mathematics, Liverpool John Moores University, James Parsons Building, Byrom Street, Liverpool, L3 3AF, UK.

[†]EPSRC Liverpool Centre for Mathematics in Healthcare, Department of Mathematical Sciences, University of Liverpool, Liverpool, L69 7ZL, UK.

[‡]MRC Centre for Inflammation Research, Queens Medical Research Institute, University of Edinburgh, 47 Little France Crescent, Edinburgh, EH16 4TJ, UK.

¹To whom correspondence should be addressed at Department of Mathematical Sciences, University of Liverpool, Peach Street, Liverpool, L69 7ZL, UK. Tel: +44 151 794 4049. E-mail: j.leasedale@liverpool.ac.uk.

²Both authors contributed equally.

Conflict of interest

The authors declared no competing interests for this work.

Funding

CLM acknowledges funding support from the Faculty of Engineering and Technology, Liverpool John Moores University. JL acknowledges funding support from the Liverpool Centre for Mathematics in Healthcare (EPSRC grant: EP/N014499/1).

Keywords

APAP, DILI, HMGB1, K18, *in-silico*, pharmacokinetics

Abstract

Paracetamol (acetaminophen, APAP) is one of the most commonly used analgesics in the UK and USA. However, exceeding the maximum recommended dose can cause serious liver injury and even death. Promising APAP toxicity biomarkers are thought to add value to those used currently and clarification of the functional relationships between these biomarkers and liver injury would aid clinical implementation of an improved APAP toxicity identification framework. The framework currently used to define an APAP overdose is highly dependent upon time since ingestion and initial dose - information which is often highly unpredictable. A pharmacokinetic-pharmacodynamic (PK-PD) APAP model has been built in order to understand the relationships between a panel of biomarkers and APAP dose. Visualisation and statistical tools have been used to predict initial APAP dose and time since administration. Additionally, logistic regression analysis has been applied to histology data to provide a prediction of the probability of liver injury.

1 Introduction

2 Acetaminophen (paracetamol, APAP) is the most commonly used painkiller in the world (1)
3 and the leading cause for acute liver failure (ALF) in the Western world (2). The current
4 antidote used to treat cases of APAP overdose, N-acetylcysteine (NAC), reduces the
5 likelihood of progression into drug-induced liver injury (DILI) (3). NAC is highly effective
6 when administered within 8 to 10 hours of initial APAP dose (4). Although NAC is currently
7 the most effective APAP overdose treatment, there are many adverse side effects such as
8 rash, vomiting and anaphylactoid reaction (3). The decision to administer NAC is currently
9 based upon the nomogram treatment line (5) which is influenced by a measurement of
10 Alanine Aminotransferase (ALT), but is also heavily dependent on the initial dose amount
11 and time elapsed since ingestion (6), information which is often highly unpredictable within
12 the clinical setting.

13 ALT elevation represents probable liver-injury post-occurrence (7) and is the most widely
14 used blood-based biomarker for measuring DILI (8). Aspartate Aminotransferase (AST) is
15 another DILI biomarker (8) that accumulates in the blood due to liver damage, but it is also
16 linked to other pathologies, e.g. heart injury (9). Increased serum total bilirubin (TBL) is
17 indicative of the substantial loss of functional hepatocytes; therefore, similar to ALT, this
18 biomarker does not predict hepatotoxicity potential but instead is a post-occurrence indicator
19 (7). In order to improve the treatment of APAP-induced DILI via NAC therapy, biomarkers
20 are required which can predict liver damage *a priori*. Although there are clear limitations,
21 clinics currently analyse changes in ALT, AST and TBL in combination to predict DILI (10).
22 Recently, biomarkers K18 and HMGB1 have been shown to add value to the measurement
23 of ALT (11) and have the potential to predict DILI pre-occurrence. However, such new
24 biomarkers are often examined singly and clarification of their functional relationships is
25 required to aid clinical implementation (12). For a thorough review of the mechanisms of DILI
26 see, for example, (13).

In-silico modelling allows for the development of mechanistic understanding of biological systems which may not always be possible from *in-vitro/in-vivo* experiments alone. An interdisciplinary, systems toxicology approach is a cost-effective way of understanding and predicting drug efficacy and toxicology whilst complying with the 3R's (scientific framework for use of animals in research) (14). There have been multiple *in-silico* models which have been previously developed to study APAP metabolism and associated toxic potential. Reith et al. (2009) produced a system of equations with parameters fitted to human data consisting of patients dosed with pain-relief to provide clarification of the role of the glucuronidation and sulphation pathways, providing a basis for examining APAP metabolism in various disease states. Ochoa et al. (16) took a multi-scale approach by firstly creating a spatiotemporal prediction of drug and metabolite concentrations within the liver, and then, at the whole-body level, including blood-flow between organs. Remien et al. (17) created a model for acetaminophen-induced liver damage and derived ordinary differential equations (ODEs) describing changes in AST, ALT and INR. The authors optimised initial APAP dose amount and time since overdose by fitting the resulting ODEs to clinical data (from 53 overdose patients). Remien et al. (18) then extended this framework to a cell-based model. Our study extends Remien's approach by combining ALT with additional biomarkers that have the potential to predict APAP-induced liver injury pre-occurrence. Additionally, the study is extended to non-overdose and overdose cases in an attempt to identify the key biomarkers that discriminate between the two situations. Ben-Shachar et al. (18) created a retrospective study complementary to Remien's model. Whilst Remien's model aimed to predict overdose occurrence, Ben-Shachar's model was used to determine whether an overdose would lead to fatal liver damage. Reddyhoff et al. (20) constructed a cell-based model that described major pathways impacting on APAP clearance. Sensitivity analysis determined which parameters had the largest effect on the progression to toxicity. Shoda et al. (21) mechanistically modelled the biomarker HMGB1. Their focus was the role of HMGB1 with regards the innate immune response and concluded that HMGB1 was a key input for immune cell activation.

In this report, our focus is to investigate HMBG1 within a panel of DILI biomarkers, attempting to predict APAP toxicity in mice. We propose a novel framework to predict initial APAP dose, time since administration and the probability of APAP-induced liver injury. The platform is distinctive primarily due to the use of promising biomarkers, optimised within the PK/PD framework by combining the use of deterministic modelling with statistical analysis. The mouse is widely considered to be a good model for APAP toxicity prediction in humans (22) and we have utilised mouse-derived data in this study to develop our new *in-silico* framework by exploiting the rich data sets available and also to avoid, at this early stage of model development, the uncertainties associated with APAP human overdose data. Translation to the human clinical case would be, in theory, a relatively simple adjustment of the PK/PD model parameters, which could be estimated from a Population-Pharmacokinetics (Pop-PK) analysis of clinical overdose data (23). However, the key feature of this current work is to demonstrate the development and validation of our new predictive framework using the more amenable mice data. The results from our investigation define currently undocumented PK parameters for APAP in mice, and the biomarkers are examined as a panel, rather than individually. Additionally, the focus of this work is the biomarkers that work well for DILI prediction due to APAP, which may only represent certain pathways or mechanisms that are not applicable to other drugs but we anticipate that this *in-silico* approach can be translated across drug space with the necessary biomarker data.

Methods

Model development (i) – APAP pharmacokinetics

Four datasets from two separate published studies (24,25) recording APAP concentration over time in mice following intraperitoneal administration of 50, 150, 500 and 530 mg/kg doses were used to parameterise a two-compartment pharmacokinetic (PK) model describing APAP metabolism in mice. Note that for applications to oral administration, the

absorption rate parameter, k_a , would be multiplied by a bioavailability fraction to implicitly take into account effects of gastric emptying and absorbed fraction (details of the model selection can be found in the supplementary material).

Two ordinary differential equations (ODEs) were used to represent changes in APAP concentration within two PK compartments (central and peripheral) of the mice in the following system,

$$\frac{dC_c}{dt} = \frac{k_a D_0 e^{-k_a t}}{V_c} + k_{21} C_p \frac{V_p}{V_c} - k_{12} C_c - k_{el} C_c, \quad (1)$$

$$\frac{dC_p}{dt} = k_{12} C_c \frac{V_c}{V_p} - k_{21} C_p, \quad (2)$$

where C_c represents the central compartment concentration of APAP ($\mu\text{mol/l}$), C_p represents the peripheral compartment concentration of APAP ($\mu\text{mol/l}$), k_a represents the absorption rate from the peritoneal cavity (h^{-1}), D_0 represents initial dose (mg), k_{21} represents the transfer rate from the peripheral to the central compartment (h^{-1}), k_{12} represents the transfer rate from the central to the peripheral compartment (h^{-1}), V_p represents the theoretical volume of the peripheral compartment (l/kg), V_c represents the theoretical volume of the central compartment (l/kg), k_{el} represents the overall elimination rate (summation of both excretion and metabolism processes) (h^{-1}), and t represents the time variable (h).

Solving both equations analytically through Laplace transforms (26) gives the following equation for paracetamol concentration in the central compartment as a function of time,

$$C_c(t) = \frac{k_a D_0}{V_c} \left[\frac{(k_{21} - \alpha)}{(k_a - \alpha)(\beta - \alpha)} e^{-\alpha t} + \frac{(k_{21} - \beta)}{(k_a - \beta)(\alpha - \beta)} e^{-\beta t} + \frac{(k_{21} - k_a)}{(\alpha - k_a)(\beta - k_a)} e^{-k_a t} \right], \quad (3)$$

where α and β are related to the model parameters as follows,

$$\alpha = \frac{1}{2} \left(k_{12} + k_{21} + k_{el} + \sqrt{(k_{12} + k_{21} + k_{el})^2 - 4k_{21}k_{el}} \right),$$

1 and

$$\beta = \frac{1}{2} \left(k_{12} + k_{21} + k_{el} - \sqrt{(k_{12} + k_{21} + k_{el})^2 - 4k_{21}k_{el}} \right).$$

2 Equation (3) was fitted to the four aforementioned datasets simultaneously using a Nelder-
3 Mead search algorithm (27), with parameters k_a, k_{21}, V_c, α and β being optimised in order to
4 minimise the difference between the model output and the observed APAP dynamics. Note
5 that all subsequent data fitting also employs this algorithm. Data fitting was performed using
6 the `fminsearch` tool in Matlab (28). Optimised parameter values and model simulation code
7 are provided in the supplementary material.

8 **Model development (ii) – glutathione depletion**

9 The role of glutathione (GSH) in APAP metabolism is to detoxify N-acetyl-p-
10 benzoquinoneimine (NAPQI), a highly reactive metabolite (13) formed following the
11 bioactivation of APAP. Therefore, GSH stores are depleted in the case of an overdose and
12 NAPQI accumulates, eventually causing liver damage. In our model, paracetamol biomarker
13 response dynamics were assumed to be directly dependent on GSH depletion. The GSH
14 parameter values were optimised such that the solution was fitted to GSH time-course data
15 from a literature study (25). GSH dynamics are described in the equation below,

$$\frac{d[gsh]}{dt} = k_o \cdot gsh_0 - k_o \cdot gsh - \frac{\xi \cdot k_{el} \cdot C_c \cdot gsh}{gsh + k_{pr}}, \quad (4)$$

16 where k_o is the basal removal rate (including background usage) of GSH (h^{-1}), gsh_0 is the
17 baseline value of GSH ($\mu\text{mol/l}$) in the APAP-free steady state, ξ is the proportion of
18 eliminated APAP that is transformed into NAPQI, and k_{pr} is the ratio of NAPQI forming other
19 protein adducts relative to NAPQI detoxified by GSH. The APAP elimination rate, k_{el} , was
20 identified during PK model development (above) whilst all other parameters were optimised
21 by fitting Equation (4) to the data in Antoine et al. (25). Further information, and full
22 derivation of the GSH ODE in Equation (4), is described in the supplementary material.

Model development (iii) – pharmacodynamics

The toxic response to APAP overdose was mathematically described with individual pharmacodynamic (PD) models representing biomarker concentrations (r = ALT, HMGB1, K18 and Fragmented K18) over time, as described in Equation (5),

$$\frac{dr}{dt} = r_0 k_{out} \left(\frac{R_{50}^n + gsh_0^n}{R_{50}^n} \right) \left(1 - \frac{gsh^n}{R_{50}^n + gsh^n} \right) - k_{out} r, \quad (5)$$

where r_0 is the biomarker baseline concentration, k_{out} is the natural decay rate of the biomarker (h^{-1}), R_{50} represents the concentration of (GSH) which causes the biomarker production (response) to be half its maximal value ($\mu\text{mol/l}$), and n is a parameter that reflects the steepness of the biomarker production term (29). Further model details can be found in the supplementary material. Whilst parameter values r_0 and gsh_0 can be identified directly from the data, k_{out} , R_{50} and n were optimised by individually fitting the model output to data measuring biomarker concentration over time following a 530 mg/kg dose of APAP (25).

Model validation

The parameterised PK-PD model was validated against data from a separate experiment (detailed below). The PK-PD model simulated several dosing scenarios [0,150,300,530] mg/kg and biomarker concentration outputs were extracted at 5 hours and compared to the experimental data. Further details and results can be found in the supplementary material (see Figure S1).

Experimental animal treatment

The protocols described were undertaken in accordance with criteria outlined in a license granted under the Animals (Scientific Procedures) Act 1986 and approved by the University of Liverpool Animal Ethics Committee. Groups of six individual CD-1 male mice (25-35 g) with free access to food and water were included in the study. For the biomarker time-course, treatment was as previously described (25). For the dose/response data used for

validation, study animals were administered either a 150, 300 or 530 mg/kg i.p APAP injection and were euthanized 5 h post-treatment. The 5 h time-point has been used in previous studies (25), and was chosen here not only because the pathological and biomarker response has been extensively categorised at this point, but the majority of key mechanisms (apoptosis, necrosis and inflammation) are also identifiable at this time-point. Control animals received either 0.9% saline or solvent control in 0.9% saline as appropriate. Serum ALT activity, HMGB1 and fragmented K18 levels were determined, and GSH content assessment was carried out on the livers of all animals. Total hepatic glutathione (GSH and oxidized glutathione) levels and biomarker quantification/characterisation were determined as described previously (25,30).

Predicting time since administration and initial dose

Multiple linear regression

The *in-silico* model was used to create virtual datasets for testing and validation (methodology in supplementary material). A robust multiple linear regression model (31) was fitted to the *in-silico* derived data to predict time since administration and initial dose.

Visualisation

Principal component analysis (PCA) (32) and the T-SNE method (33) were applied to visualise the simulated *in-silico* datasets with regards to linear combinations of all variables (APAP and toxicity biomarkers combined) for each *in-silico* individual.

Classification

Appropriate classes for each dose and time range were identified to see if the time-since-administration and dose amount could be predicted for a new individual within the population. Various classification techniques (detailed in supplementary material) appropriate for such a task were used and compared.

1

2 ***Predicting probability of liver injury***

3 The biomarker time-course experimental data used to create the PD model (25) also
4 provided a corresponding histology score for each mouse from the range [0, 1, 2, 3]. These
5 histology scores were binarised based upon previously published criteria (25). Forward-
6 stepwise binary logistic regression (34) was applied in order to understand the most
7 significant biomarker, or panel of biomarkers for DILI. The most significant biomarkers were
8 then used in combination with PK-PD model simulations to predict the DILI probability (35).

9 Further details of all aforementioned statistical techniques can be found in the
10 supplementary information.

11

12 **Results**

13 Results from the parameter optimisation of the PK-PD models can be seen in Figure 1. Note
14 that sufficient early time experimental APAP plasma concentrations are currently unavailable
15 which would verify the accuracy of T_{max} and C_{max} of the 530-mg dose. Nevertheless, with a
16 R^2 value of 0.8304 for the PK model, and values of 0.7513, 0.9634, 0.7413, and 0.6526 for
17 the PD models for ALT, HMGB1, K18 and fragmented K18 respectively, it is shown that the
18 *in-silico* model recapitulates *in-vivo* experimental dynamics. Optimised parameters for all of
19 the PK-PD models can be found in the supplementary material (Table S1).

20 The R_{50} parameter in the biomarker PD models defines a concentration of GSH at which the
21 biomarker has reached half of its maximal production rate (MPR). For biomarkers ALT,
22 HMGB1, K18 and fragmented K18, the R_{50} values were 227.67, 399.08, 212.87 and 72.09
23 $\mu\text{mol/L}$ respectively. Therefore, in the model, as GSH is depleted from a baseline of 696.91
24 $\mu\text{mol/L}$ (36) and reaches a concentration 399.08 $\mu\text{mol/L}$ (42.73% depletion), HMGB1 has
25 reached half of its MPR and is therefore considered to be the fastest responding biomarker.

GSH must be further depleted to 227.67 $\mu\text{mol/L}$ and 212.87 $\mu\text{mol/L}$ (67-69% depletion), respectively, before biomarkers ALT and K18 reach half of their MPR. Approximately 90% GSH depletion is required for fragmented K18 to reach half of its MPR in the model.

Identifying time/dose category following APAP dose

Projecting the *in-silico* derived data on to the principal components and visualising with respect to time since administration and dose amount, as can be seen in Figure 2 (a)-(b), allowed classes to be clearly distinguished with minimal level of overlap confirming the biomarker utility in class prediction. The level of class overlap with respect to dose is significantly lower. Visualising the data with the T-SNE method (Figure 2 (c)-(d)) enhances the previous visualisation, in that dose may be separated more accurately. Additionally, the time-since-administration classes are more separable with the T-SNE method, particularly with earlier time ranges.

The classification results are consistent across the different methodologies (Table 1). Should a new observation arise, this framework could predict which 'time-since-administration' and 'dose' category it should be placed in with 73.7% and 86.5% accuracies respectively. The results of the linear regression model used to evaluate time since administration and initial dose, both as continuous variables, are reported in Table 2. In both cases, the model is significant at the 99% confidence level. The R^2 values indicate that when predicting time since administration, approximately 53% of the variance in results can be explained by the model, whilst when predicting dose approximately 80% of the variation can be explained by the model. An exact time-since-administration value was able to be predicted with a residual standard error and accuracy of 3.6 h, whilst an exact dose was predicted with only an error of 56.81 mg/kg.

Predicting the probability of liver injury following an APAP dose

From the forward-stepwise logistic regression analysis, the model which used HMGB1 concentration alone as a predictor had the highest significance (p-value 0.003). Figure 3 (a)-

(f) represents the fold-changes in biomarker concentrations with respect to time following various doses. For higher doses, APAP and related toxicity biomarker concentrations are significantly increased during the time course, whilst GSH is significantly decreased at higher doses, representing depletion of stores. Figure 3 (g) shows how the probability of serious liver injury (dependent only on HMGB1 concentration as predicted by the logistic regression model) changes over time for doses between 0-600 mg/kg. A threshold probability of 0.5 (i.e. 50% liver injury likelihood) was used to determine likeliness of DILI. Any observation within the white contour boundary is therefore predicted likely to be a concentration representative of liver injury (i.e. 50% chance). For lower toxic doses, according to the model, HMGB1 concentrations that likely indicate liver injury are most apparent between 5-10 h post-dose. As the dose increases, the time-frame increases to approximately 5-15 h. Note that combinations of APAP/ALT and APAP/Full K18 were also significant; therefore, these biomarker combinations could be investigated in the case of predicting DILI following late presentation of paracetamol toxicity and prognosis within the 24 h window.

Currently, toxicity is thought to be apparent in mice after a 300 mg/kg dose, shown by the red line in Figure 3 (g). Our binary logistic regression (model based solely on HMGB1 concentration) states there is more than 50% chance of liver injury at a 200 mg/kg dose, shown by the white contour in Figure 3 (g). The currently used toxic dose (300 mg/kg) coincides with around 90% GSH depletion which can be seen in Figure 3 (b). This coincides with a relationship well known in the literature (13). This toxic level is also the dose at which fragmented K18 begins to elevate, as shown in Figure 3 (f). The toxic dose proposed by the *in-silico* model (200 mg/kg) is the dose at which ALT and full K18 begin to elevate (Figure 3 (c) and Figure 3 (e) respectively) and HMGB1 first reaches peak concentration (Figure 3 (d)).

Visualising the probability of liver injury following an APAP dose

Combining the PCA/T-SNE analysis with our proposed framework for predicting the probability of liver injury allowed the virtual datasets to be visualised not only with regard to the initial dose and time since ingestion, but also the subsequent probability of liver injury. With reference to Figure 4, observations with a high probability of liver injury are clearly clustered within the parameter space and separable from low probability cases. Additional similar projections (with both the PCA and T-SNE methods), including the estimated maximum probability of liver injury for each observation, are shown in the supplementary material.

Discussion

The current clinical framework for predicting whether or not APAP antidote treatment is necessary is highly dependent upon information provided by the patient such as when the dose was taken and in what quantity. This information is often vague and/or unreliable. Consequently, critically vulnerable patients are often left untreated or, conversely, NAC is unnecessarily administered. Changes in legislation have already led to an estimated increased cost of £8.3 million per year due to overused NAC treatment (37). Mathematical and statistical analysis provide a proof-of-concept tool to predict information with a much higher level of certainty, based on a panel of promising biomarkers.

We have developed an optimised PK-PD model for APAP and appropriate biomarkers of liver injury in a systems toxicology approach. The model was used to conduct investigations within a dosing range of 0-600 mg/kg without any further *in-vivo* testing. The optimised *in-silico* framework is suitable for use in further theoretical investigations, providing greater scope for reducing the dependency on animal testing in toxicity and complying with 3Rs principles (14). For example, results from our analysis could improve experimental refinement such as predicting the probability of liver injury and toxicity at 200 mg/kg in mice

rather than 300 mg/kg. Not only may experimentalists be dosing mice at amounts higher than necessary, they may also be missing vital information apparent at lower doses.

APAP-induced liver toxicity is thought to occur when GSH depletes by around 80-90% (13), which coincided with elevated fragmented K18 levels. The *in-silico* PD model, and its reported R_{50} values, suggest that levels of HMGB1, ALT and Full K18 elevate prior to this depletion level, elevating at 43%, 67% and 69% respectively. As a result, HMGB1 in particular could be considered as an earlier indicator of DILI.

The identification of more accurate predictions of dose timing and amount, informed by biomarker concentration samples, will improve nomogram treatment line accuracy (6). Predictions for the time since administration were successfully categorised into (0-2], (2-5], (5-10], (10-15], and (15-24]-hour ranges based on APAP, ALT, HMGB1 and full K18 concentration values with 73.7% accuracy. Should this framework be translated to a similar level of efficiency in the human clinical case, this information will have impact regarding the determination of the potential liver injury, with less dependency on patient information. Additionally, an exact value was predicted with an accuracy of 3.6 h. Similarly, initial dose was able to be classified into [0-200], [201-400], [401-600] mg/kg categories with 86.5% accuracy and an exact dose predicted with an expected error of ± 56.81 mg/kg. A panel of biomarker measurements could be used in this manner to provide the dose and time information, which will identify a (time-dose) point on the liver injury framework, provided in Figure 3-G, from which one can read off an instantaneous probability of liver injury and how this probability is predicted to change as time progresses. Obtaining dose and time information based on biomarker concentrations and combining this with our proposed liver injury framework shows the utility of these biomarkers in predicting dose amount, time since ingestion and the subsequent probability of liver injury.

Although ALT concentration is currently used as a clinical measure to inform potential toxicity, it was found to have the least importance in the regression model for predicting time

1 since administration as a continuous variable. Out of all the biomarkers used in the multiple
2 linear regression analysis, HMGB1 was found to have the highest time-since-administration
3 model coefficient. This analysis suggests therefore, that not only is HMGB1 an earlier
4 indicator of DILI, but it is also an important biomarker in accurately predicting the time
5 elapsed since administration. Furthermore, logistic regression analysis identified HMGB1 as
6 the most significant predictor for liver injury, in line with recent studies defining HMGB1 as a
7 more sensitive DILI predictor (38). As noted above, the focus of this work has been the
8 biomarkers that work well for DILI prediction due to APAP, in which case HMGB1 is
9 highlighted by our analysis. However, for different drugs, DILI may involve different
10 mechanisms and, as such, HMGB1 may not perform so well as a singular biomarker but
11 instead a panel would be more predictive.

12 While the results from the T-SNE method for visualisation showed clear separation,
13 particularly with regards to the probability of liver injury, there was a slight overlap in the
14 time-since-administration and dose plots. This result supports the possibility of defining
15 further classes through unsupervised methodologies in future investigations. The
16 classification techniques used provided incredibly high accuracy levels considering the
17 nature of the problem. A further investigation of interest is the rate of misclassification
18 between the classes with regard to critical errors at the edges of the variable ranges.

19 The framework proposed has the potential for substantial clinical impact once translated to
20 human. The analysis was applied to mice due to the relative abundance and quality of data
21 (especially for toxicity cases) and the quantity of relevant biomarker data required to properly
22 characterise such a mathematical and statistical predictive framework. Equivalent APAP
23 clinical data is available but has a tendency to be noisy, sparse and inconsistent. Analysis of
24 such data would therefore require the significant application of (top-down) Population-
25 Pharmacokinetics (Pop-PK) to unravel the stochasticity of the mixed-effects involved, in
26 addition to understanding and capturing the mechanisms of the PK-PD problem. For
27 example, the relative influence of variation in certain model parameters on quantitative

1 model outputs can be determined by sensitivity analysis, allowing for identification of
2 mechanistic processes that would require particularly careful consideration when translating
3 this model to a human clinical Pop-PK framework (see supplementary information for further
4 details).

5 An advantage of our study is that the same biomarkers can be measured in both humans
6 and animals by the same methodologies. Moreover, the model hepatotoxin we have
7 employed, acetaminophen, is directly comparable between human and mice with respect to
8 mechanism of toxicity and action of the antidote. The major differences between human and
9 mouse studies are the mass dose of acetaminophen needed to induced toxicity in mice and
10 the kinetics of the biomarker profile (25,39,40). The dose response in mice is well
11 documented and is consistent with our data. Furthermore, this can be adjusted as a
12 parameter within our model to reflect the clinical situation. There are a number of clinical
13 studies now published that have measured these biomarkers from human studies in a time-
14 dependent way (41,42). The approach we describe to modify dose adjustment can also be
15 undertaken to reflect biomarker kinetic differences. It is important to note that it is difficult to
16 properly obtain or assess human pathology in the acute setting, and it is only really in the
17 event of liver transplantation that we see a strong relationship between human and mouse
18 (25,43). Given the strong relationship between the biomarker signatures and mechanism of
19 APAP action between human and mouse, it would be reasonable to translate findings from
20 mouse acute data (25,39), to human acute data (11). Taking these points into consideration,
21 in its current form, our framework is highly predictive and provides promise for clinical use in
22 discriminating time since administration, initial dose amount and subsequent probability of
23 liver injury. This would be a significant application and could instruct the determination of
24 NAC intervention in patients suspected of APAP overdose.

25 Clinical assessment of DILI is, in practice, often based on causality assessment, with expert
26 opinion being the gold standard and does not wholly depend on simple biochemical tests.
27 We have recently discussed the potential improvement to lab-based measures in aiding DILI

assessment and one key feature we propose is that lab measurements should be repeated when DILI is suspected (11,44). This could allow for the determination of the cause of injury as well as the derivation of the AUC of a liver toxicity marker. A limitation of our current *in-silico* model framework is that it is focused on whether or not liver injury occurs, rather than prediction of the maximum damage observed in an individual. The cause of this limitation is the sparsity of the histology data used for model parameterisation. However, if such additional AUC-based measurements could be obtained then this could potentially offer vital data to extend the predictive potential of our *in-silico* platform by quantifying the maximal liver injury and further aiding DILI assessment.

Study Highlights

What is the current knowledge on the topic?

The current clinical framework for predicting paracetamol overdose is imprecise, predominantly due to a dependency on uncertain information from patients such as dose amount and time since administration.

What question did this study address?

Mathematical modelling and statistical methods are applied to predict dose, time since administration and the probability of paracetamol-induced-liver-injury based on biomarker information by exploiting the relative abundance and quality of mouse data.

What does this study add to our knowledge?

A new *in-silico* paracetamol toxicity identification framework is described to simulate the pharmacokinetic/pharmacodynamic behaviour of paracetamol and a panel of corresponding toxicity biomarkers with considerable translational potential.

How might this change drug discovery, development, and/or therapeutics?

1 Systems toxicology approaches to direct biomarker identification and optimisation can also
2 be used to develop predictive modelling frameworks for other hepatotoxic drugs. An
3 understanding of complex biological system interactions is required to refine potential
4 treatment strategies and improve safety, ethics and cost-efficiency. Mathematical modelling
5 provides an enhanced mechanistic understanding while statistical modelling can provide
6 robust, physiologically relevant predictions to underpin future investigations.

7 **Acknowledgements**

8 CLM acknowledges funding support from the Faculty of Engineering and Technology,
9 Liverpool John Moores University. JL acknowledges funding support from the Liverpool
10 Centre for Mathematics in Healthcare (EPSRC grant: EP/N014499/1).

11 **Author Contributions**

12 C.L.M., J.L., and S.D.W. wrote the manuscript; D.J.A. and S.D.W. designed the research;
13 C.L.M., J.L., and S.D.W. performed the research; C.L.M., S.T. and I.J. analyzed the data.

References

1. Chiew A, Fountain J, Graudins A, Geoffrey KI, Reith D, Buckley NA. Guidelines for the management of paracetamol poisoning in Australia and New Zealand (web). Med J Aust [Internet]. 2015 [cited 2017 May 12]; Available from: https://www.mja.com.au/sites/default/files/issues/203_05/Guidelines_paracetamol_Aus_NZ_2015.pdf
2. Larson AM, Polson J, Fontana RJ, Davern TJ, Lalani E, Hynan LS, et al. Acetaminophen-induced acute liver failure: Results of a United States multicenter, prospective study. Hepatology. 2005;42(6):1364–1372.
3. Antoine DJ, Dear JW. How to treat paracetamol overdose and when to do it. Expert Rev Clin Pharmacol [Internet]. 2016;9(5):633–5. Available from: <http://www.ncbi.nlm.nih.gov/pubmed/26881838>
4. Juurlink D. Drug-Induced Hepatotoxicity. N Engl J Med [Internet]. 2003 [cited 2017 Apr 26];349:1974–6. Available from: <http://www.nejm.org/doi/pdf/10.1056/NEJM200311133492021>
5. Rumack B, Peterson R, Koch G, Amara I. Acetaminophen overdose. 662 cases with evaluation of oral acetylcysteine treatment. Arch Int Med. 1981;141(3):380–5.
6. GlaxoSmithKline. Guidelines for the management of paracetamol overdose [Internet]. <http://www.asem.org.au/document.php/njxudmy/Paracetamol+Overdose+Treatment+Nomogram.pdf>. 2007 [cited 2017 Apr 10]. Available from: <http://www.asem.org.au/document.php/njxudmy/Paracetamol+Overdose+Treatment+Nomogram.pdf>
7. Clarke J, Dear J, Antoine DJ. Recent advances in biomarkers and therapeutic interventions for hepatic drug safety - false dawn or new horizon? Expert Opin Drug Saf. 2016;

8. BritishLiverTrust. Liver Function Tests [Internet]. 2017 [cited 2017 May 5]. Available from: <https://www.britishlivertrust.org.uk/liver-information/tests-and-screening/liver-function-tests/>
9. Giannini EG, Testa R, Savarino V. Liver enzyme alteration: A guide for clinicians. *Cmaj*. 2005;172(3):367–79.
10. FDA. Guidance for Industry Drug-Induced Liver Injury: Premarketing Clinical Evaluation. *Drug Saf* [Internet]. 2009;(July):28. Available from: <https://www.fda.gov/downloads/drugs/guidancecomplianceregulatoryinformation/guidances/ucm174090.pdf>
11. Antoine DJ, Dear JW, Lewis PS, Platt V, Coyle J, Masson M, et al. Mechanistic Biomarkers Provide Early and Sensitive Detection of Acetaminophen-Induced Acute Liver Injury at First Presentation to Hospital. *Hepatology* [Internet]. 2013 [cited 2017 Apr 26];58(2):777–87. Available from: <https://www.ncbi.nlm.nih.gov/pmc/articles/PMC3842113/pdf/hep0058-0777.pdf>
12. Beger RD, Bhattacharyya S, Yang X, Gill PS, Schnackenberg LK, Sun J, et al. Translational biomarkers of acetaminophen-induced acute liver injury. *Arch Toxicol*. 2015;89(9):1497–522.
13. Hinson JA, Roberts DW, James LP. Mechanisms of Acetaminophen-Induced Liver Necrosis. *Pharmacology* [Internet]. 2010;196(196):1–34. Available from: <http://www.springerlink.com/index/10.1007/978-3-642-00663-0>
14. NC3Rs. The 3Rs [Internet]. 2017 [cited 2017 Apr 28]. Available from: <https://www.nc3rs.org.uk/the-3rs>
15. Reith D, Medlicott NJ, Kumara De Silva R, Yang L, Hickling J, Zacharias M. Simultaneous modelling of the michaelis-menten kinetics of paracetamol sulphonation and glucuronidation. *Clin Exp Pharmacol Physiol*. 2009;36(1):35–42.

- 1 16. Diaz Ochoa JG, Bucher J, Péry ARR, Zaldivar Comenges JM, Niklas J, Mauch K. A
2 multi-scale modeling framework for individualized, spatiotemporal prediction of drug
3 effects and toxicological risk. *Front Pharmacol*. 2014;4 JAN(January):1–11.
- 4 17. Remien CH, Adler FR, Waddoups L, Box TD, Sussman NL. Mathematical modeling of
5 liver injury and dysfunction after acetaminophen overdose: Early discrimination
6 between survival and death. *Hepatology*. 2012;56(2):727–34.
- 7 18. Remien CH, Sussman NL, Adler FR. Mathematical modelling of chronic
8 acetaminophen metabolism and liver injury. *Math Med Biol*. 2014;31(3):302–17.
- 9 19. Ben-Shachar R, Chen Y, Luo S, Hartman C, Reed M, Nijhout HF. The biochemistry of
10 acetaminophen hepatotoxicity and rescue: a mathematical model. *Theor Biol Med*
11 *Model* [Internet]. 2012;9:55. Available from:
12 [http://www.pubmedcentral.nih.gov/articlerender.fcgi?artid=3576299&tool=pmcentrez&](http://www.pubmedcentral.nih.gov/articlerender.fcgi?artid=3576299&tool=pmcentrez&rendertype=abstract)
13 [rendertype=abstract](http://www.pubmedcentral.nih.gov/articlerender.fcgi?artid=3576299&tool=pmcentrez&rendertype=abstract)
- 14 20. Reddyhoff D, Ward J, Williams D, Regan S, Webb S. Timescale analysis of a
15 mathematical model of acetaminophen metabolism and toxicity. *J Theor Biol*
16 [Internet]. 2015;386:132–46. Available from:
17 <http://dx.doi.org/10.1016/j.jtbi.2015.08.021>
- 18 21. Shoda LKM, Battista C, Siler SQ, Pisetsky DS, Watkins PB, Howell BA. Mechanistic
19 Modelling of Drug-Induced Liver Injury: Investigating the Role of Innate Immune
20 Responses. 2017;
- 21 22. Jaeschke H, Xie Y, McGill MR. Review Article Acetaminophen-induced Liver Injury :
22 from Animal Models to Humans. 2014;2:153–61.
- 23 23. Bateman DN, Dear JW, Thanacoody HKR, Thomas SHL, Eddleston M, Sandilands
24 EA, et al. Reduction of adverse effects from intravenous acetylcysteine treatment for
25 paracetamol poisoning: a randomised controlled trial. *Lancet* [Internet].

2012;383(9918):697–704. Available from: [http://dx.doi.org/10.1016/S0140-6736\(13\)62062-0](http://dx.doi.org/10.1016/S0140-6736(13)62062-0)

24. Coen M, Ruepp SU, Lindon JC, Nicholson JK, Pognan F, Lenz EM, et al. Integrated application of transcriptomics and metabonomics yields new insight into the toxicity due to paracetamol in the mouse. *J Pharm Biomed Anal.* 2004;35(1):93–105.

25. Antoine DJ, Williams DP, Jenkins AK, Regan SL, Sathish JG, Kitteringham NR, et al. High-mobility group box-1 protein and keratin-18, circulating serum proteins informative of acetaminophen-induced necrosis and apoptosis in vivo. *Toxicol Sci.* 2009;112(2):521–31.

26. Metzler CM. Open of the Two-Compartment Usefulness Model in Pharmacokinetics. *J Am Stat Assoc* [Internet]. 2012;66(333):49–53. Available from: <http://www.jstor.org/stable/2284845>

27. Wright MH. Nelder, Mead, and the Other Simplex Method. 2010 [cited 2017 May 12]; Available from: http://www.math.uiuc.edu/documenta/vol-ismp/42_wright-margaret.pdf

28. Mathworks. Matlab. Natick, Massachusetts: The MathWorks Inc.; 2016.

29. Sharma A, Jusko WJ. Characteristics of indirect pharmacodynamic models and applications to clinical drug responses. *Br J Clin Pharmacol.* 1998;45(3):229–39.

30. Williams DP, Antoine DJ, Butler PJ, Jones R, Randle L, Payne A, et al. The Metabolism and Toxicity of Furosemide in the Wistar Rat and CD-1 Mouse: a Chemical and Biochemical Definition of the Toxicophore. 2007;322(3):1208–20.

31. Ambrosius W. Multiple Linear Regression. In: *Topics in Biostatistics.* 2007. p. 165–87.

32. Jeong DH, Ziemkiewicz C, Ribarsky W, Chang R. Understanding Principal Component Analysis Using a Visual Analytics Tool. *Proc UKC 2009, Math Fundam Appl* 2009 [Internet]. 2009;1–10. Available from:

papers3://publication/uuid/F74403D9-F5D5-420C-8A62-C44E90A43EBD

33. Maaten L Van Der. Accelerating t-SNE using tree-based algorithms. 2014;15:3221–45.

34. Bewick V, Ball Jonathan. Statistics Review 14: Logistic Regression. Crit Care Febr [Internet]. 2005 [cited 2017 May 12];9(1). Available from: http://download.springer.com/static/pdf/573/art%253A10.1186%252Fcc3045.pdf?originUrl=http%3A%2F%2Fccforum.biomedcentral.com%2Farticle%2F10.1186%2Fcc3045&token2=exp=1494589205~acl=%2Fstatic%2Fpdf%2F573%2Fart%25253A10.1186%25252Fcc3045.pdf*~hmac=06e79ab0adf

35. Brannick M. Logistic Regression [Internet]. 2016 [cited 2017 Apr 28]. Available from: <http://faculty.cas.usf.edu/mbrannick/regression/Logistic.html>

36. Antoine DJ. Chemical and molecular markers of hepatic drug bioactivation, apoptosis and necrosis [Internet]. University of Liverpool; 2009. Available from: <http://ethos.bl.uk/OrderDetails.do?uin=uk.bl.ethos.501593>

37. Bateman DN, Carroll R, Pettie J, Yamamoto T, Elamin MEMO, Peart L, et al. Effect of the UK's revised paracetamol poisoning management guidelines on admissions, adverse reactions and costs of treatment. Br J Clin Pharmacol. 2014;78(3):610–8.

38. Lea JD, Clarke JI, Mcguire N, Antoine DJ. Redox-Dependent HMGB1 Isoforms as Pivotal Co-Ordinators of Drug-Induced Liver Injury: Mechanistic Biomarkers and Therapeutic Targets. Antioxidants Redox Cycl. 2016;24(12):1–45.

39. Brilliant N, Elmasry M, Burton NC, Monne J, Sharkey JW, Fenwick S, et al. Dynamic and accurate assessment of acetaminophen-induced hepatotoxicity by integrated photoacoustic imaging and mechanistic biomarkers in vivo. Toxicol Appl Pharmacol [Internet]. 2017;332:64–74. Available from: <http://dx.doi.org/10.1016/j.taap.2017.07.019>

- 1 40. Antoine DJ, Jenkins RE, Dear JW, Williams DP, Mitchell R, Sharpe MR, et al.
2 Molecular forms of HMGB1 and Keratin-18 as mechanistic biomarkers for mode of
3 cell death and prognosis during clinical acetaminophen hepatotoxicity. *Hepatology*.
4 2012;56(5):1070–9.
- 5 41. Dear JW, Clarke JI, Francis B, Allen L, Wraight J, Shen J, et al. Risk stratification after
6 paracetamol overdose using mechanistic biomarkers : results from two prospective
7 cohort studies. *Lancet Gastroenterol Hepatol* [Internet]. 2017;1253(17):1–10.
8 Available from: [http://dx.doi.org/10.1016/S2468-1253\(17\)30266-2](http://dx.doi.org/10.1016/S2468-1253(17)30266-2)
- 9 42. Longo DM, Generaux GT, Howell BA, Siler SQ, Antoine DJ, Button D, et al. Refining
10 Liver Safety Risk Assessment: Application of Mechanistic Modeling and Serum
11 Biomarkers to Cimaglermin Alfa (GGF2) Clinical Trials. 2017;102(6):961–9.
- 12 43. Bechmann LP, Marquitan G, Jochum C, Saner F, Gerken G, Canbay A. Apoptosis
13 versus necrosis rate as a predictor in acute liver failure following acetaminophen
14 intoxication compared with acute-on- chronic liver failure. *Liver Int*. 2008;28(5):713–6.
- 15 44. Antoine DJ, Ph D. Laboratory-Based Biomarkers to Improve Causality Assessment in
16 Drug-Induced Liver Injury. 2017;9(2):38–42.

Figure Legends

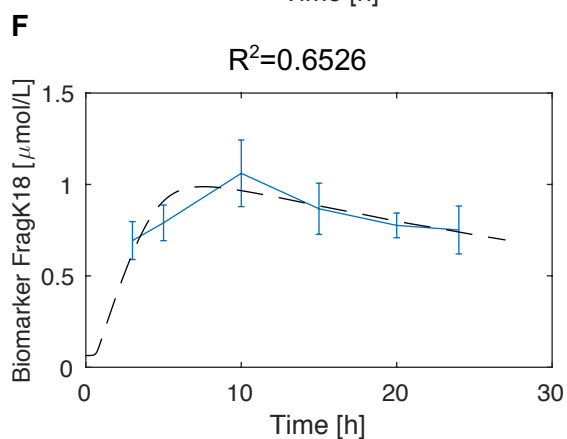
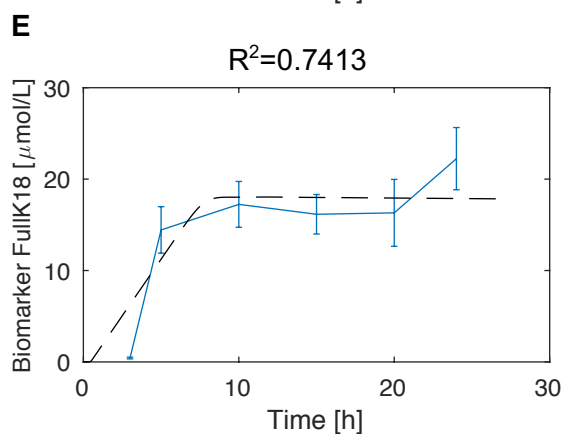
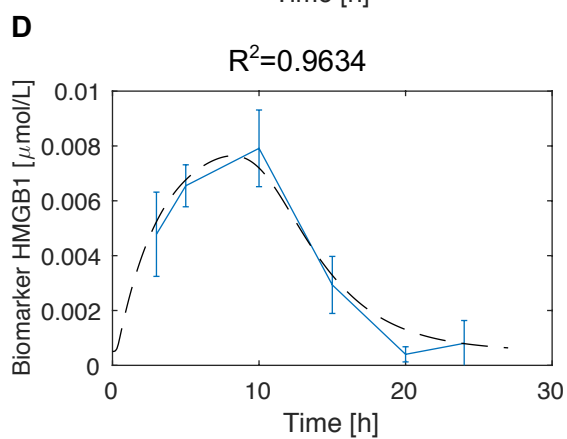
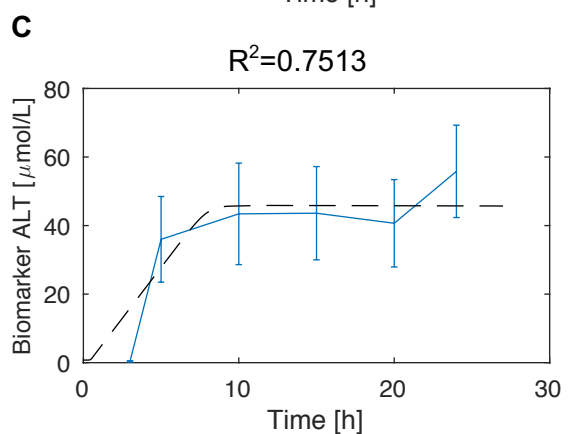
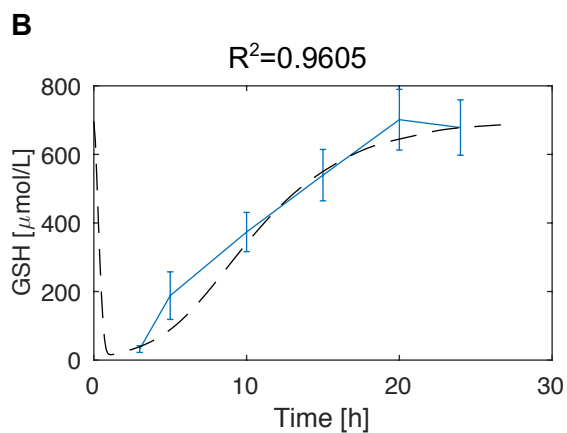
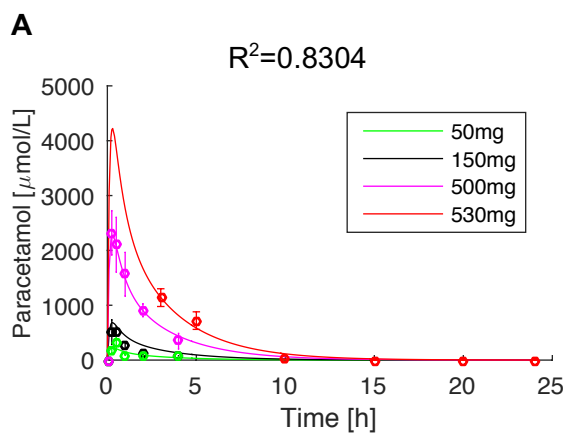
Figure 1. *In-silico* simulation outputs from the optimised model compared with the experimental data. (a) APAP PK simulations (solid lines) comparable to original data values with green, black, magenta and red representing APAP time-course following a 50, 150, 500, and 530 mg/kg dose respectively. (b) GSH simulations (black dashed lines) comparable to original data (blue). Individual PD simulation (black dashed lines) comparable to data (blue) for biomarkers ALT (b), HMGB1 (c), Full K18 (d), and Fragmented K18 (e).

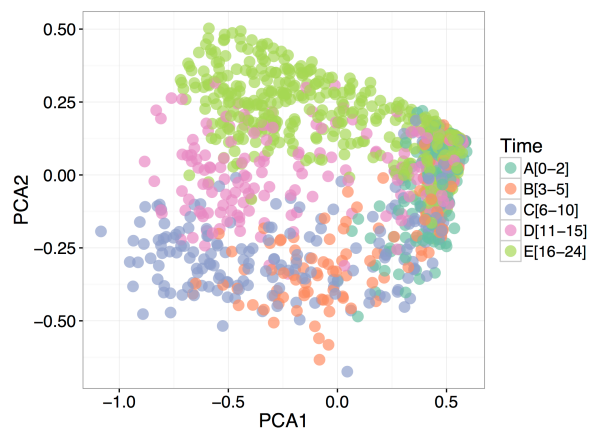
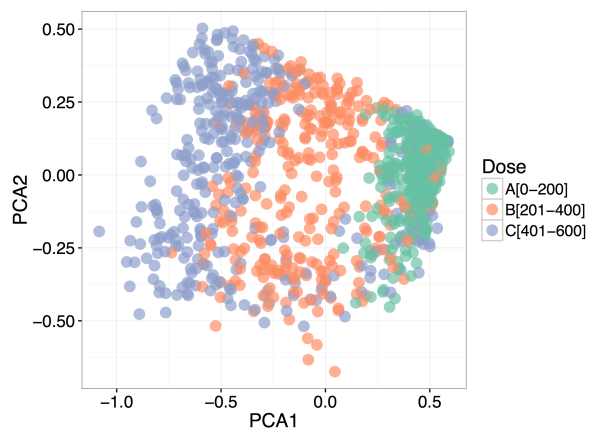
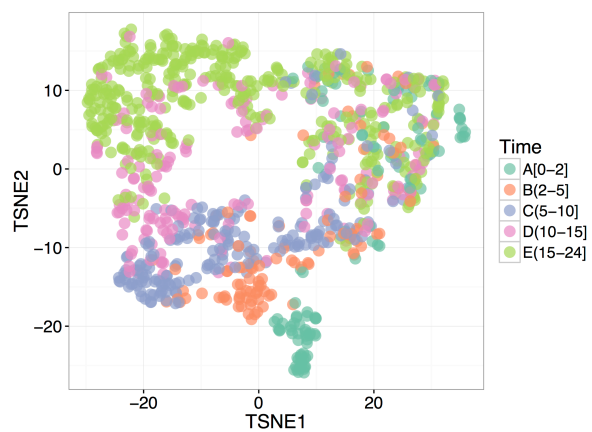
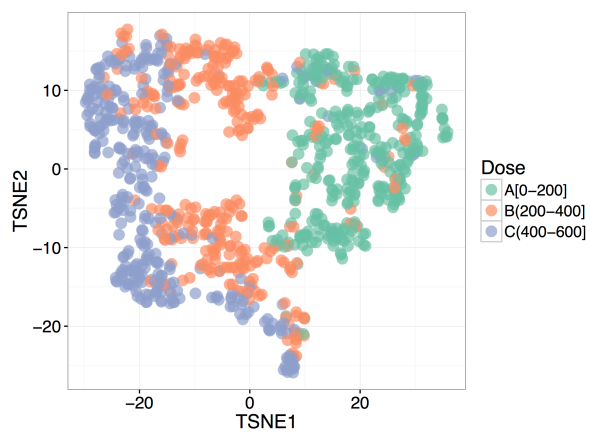
Figure 2. Visualisation and classification of time-since-administration and dose results. For time-since-administration, dark green represents class [0-2), orange represents [2-5), blue represents [5-10), pink represents [10-15) and pale green represents [15-24) hours. For dose, green represents [0-200], orange represents [201-400] and blue represents [401-600] mg/kg. (a)-(b) 2-dimensional PCA visualisation of *in-silico* mouse observations with respect to time since administration and dose respectively. (c)-(d) 2-dimensional TSNE visualisation of *in-silico* mouse observations with respect to time since administration and dose respectively.

Figure 3. (a)-(f) Fold-changes in biomarker concentration relative to their baseline values over time [0-24] hrs for APAP, GSH, ALT, HMGB1, Full K18 and Fragmented K18 respectively, following APAP doses ranging from 0-600 mg/kg. (g) Proposed framework for predicting probability of liver injury dependent upon dose, time and HMGB1 concentration. The white contour indicates the threshold of probability 0.5 of liver injury, the red dashed-line represents currently used APAP dose for toxicity studies in mice, the white dashed-line represents toxic dose proposed by our model, the green dashed-line indicates current known therapeutic dose for mice.

Figure 4: 2-dimensional TSNE visualisation of *in-silico* mouse observations with respect to estimated probability of liver injury.

- 1 **Supplemental Files**
- 2 Supplementary Material
- 3 Model Code
- 4



A**B****C****D**

Classification Method	Time Accuracy	Dose Accuracy
Multinomial Logistic Regression	0.728	0.865
Ordinal Multinomial Logistic Regression	0.570	0.859
Naïve Bayes	0.689	0.844
Linear Discriminant Analysis	0.657	0.860
Quadratic Discriminant Analysis	0.737	0.853
K-nearest neighbour	0.664	0.859
Optimal Weighted Nearest Neighbour	0.676	0.858

Table 1: Classification results for several algorithms with respect to time-since-administration and dose respectively, with numbers representing levels of accuracy. For example, the multinomial logistic regression model can predict time since administration with 72.8% accuracy.

	Dependent Variable (coefficient and related error)	
	Time (1)	Dose (2)
APAP Concentration	-18.141*** (1.095)	445.602*** (13.865)
ALT concentration	2.402** (0.988)	94.724*** (12.830)
HMGB1 concentration	-15.928*** (0.636)	
Full K18 concentration	8.964*** (0.837)	241.527*** (12.958)
Fragmented K18 concentration		310.574*** (13.260)
Constant	14.812*** (0.268)	67.068*** (3.193)
Observations	1,000	1,000
Residual Std. Error (df == 994)	3.593	56.805
<i>Note:</i> *p<0.1; **p<0.05; ***p<0.01		

Table 2: Multiple linear regression analysis results - summary statistics for models used to predict both time since administration and dose. The first number in each element of the table represents the biomarker coefficient in the regression model, whilst the second number represents the coefficient's corresponding error. For example, -18.141 is the APAP concentration coefficient in the model predicting time since administration, and this coefficient has an error of 1.095. The significance of each biomarker in the model is indicated by the number of asterisks (see note).

